Journal of Alloys and Compounds 488 (2009) 217–222

Contents lists available at ScienceDirect

Journal of Alloys and Compounds

journal homepage: www.elsevier.com/locate/jallcom

Effects of Si additions on intermetallic compound layer of aluminum–steel TIG welding–brazing joint

J.L. Song, S.B. Lin*, C.L. Yang, C.L. Fan

State Key Laboratory of Advanced Welding Production Technology, School of Materials Science and Engineering, Harbin Institute of Technology, No. 92, West Da-Zhi Street, Harbin 150001, PR China

ARTICLE INFO

Article history:
Received 15 May 2009
Received in revised form 19 August 2009
Accepted 19 August 2009
Available online 26 August 2009

Keywords:
Intermetallics
Microstructure
Mechanical properties
Liquid–solid reactions

ABSTRACT

Dissimilar metals of 5A06 aluminum alloy and AISI 321 stainless steel were butt joined successfully by TIG welding–brazing with 1100 pure Al, 4043 AlSi5 and 4047 AlSi12 filler metals. Si additions in the filler metal have great effects in preventing the growth of the IMC layer, and minimizing its thickness. The joint interface with pure aluminum consists of the θ-$FeAl_3$ in aluminum side and η-Fe_2Al_5 in steel side, while the interfaces with Al–Si filler metals are the τ_5-$Al_{7.2}Fe_{1.8}Si$ in aluminum side and θ-$Fe(Al,Si)_3$ in steel side. And with 5 wt.% of Si additions, the IMC layer has the optimum mechanical properties, and the tensile strength of the joint reaches 125.2 MPa. The growth mechanism of the IMC layers is controlled by the dissolution and diffusion of Fe atoms in the liquid. At the same time, Si atoms aggregate in the interface and participate the IMC layer's formation.

1. Introduction

In modern industry applications, e.g. automobile manufacture, shipbuilding, and aircraft construction, material combinations between aluminum alloy and steel are used to obtain a cost-favorable and weight-optimized body with a high stiffness [1]. However, joining of aluminum alloy and steel has great difficulty by fusion welding, as aluminum and steel exhibit great differences in their chemical and physical properties, and mass of brittle intermetallic compounds (IMCs) are formed seriously degrading the mechanical properties of the joints [2,3]. Thus, solid-state welding methods, e.g. explosive welding, friction stir welding and ultrasonic welding, have been used to make these dissimilar metals joint, but the shape and size of such solid-state joints are extremely restricted [4–6].

Nowadays, tungsten inert gas (TIG) welding–brazing offers a great potential for aluminum alloy and steel joining. In this process, the sheets and filler metals are heated or melted by TIG arc, and the joint has a dual characteristic: in aluminum side it is a welding joint, while in steel side it is a brazing joint [7,8]. However, Al–Fe IMC layer, e.g. Fe_2Al_5 and $FeAl_3$, formed in the brazing joint, is detrimental to the mechanical properties of the joint because it is both brittle and exists as thin plates. In aluminizing process and CMT arc joining of aluminum alloy and steel, Si additions in Al-based filler metal are used to control the growth of brittle Al–Fe IMC layer by replacing Al–Fe phases with less detrimental Al–Fe–Si phases [9,10].

However, in TIG welding–brazing process, the heating-up temperature changes quickly and the reaction time between liquid filler metal and solid steel is very short. So in such environment, effects of Si additions are different from those in aluminizing process. Until now, in TIG welding–brazing of aluminum alloy and steel, there have been few systematic studies of the IMC layers and the mechanical properties of the joint as a function of Si content in Al-based filler metal. In this study, the effects of Si on the IMC layers and the properties of the joint are reported.

2. Experimental procedures

2.1. Materials and filler metals

Materials used are 5A06 aluminum alloy and AISI 321 austenite stainless steel plates of 3.0 mm thickness. The filler metals adapted are 1100, 4043 and 4047, three kinds of aluminum based welding wires with the different contents of Si additions. The chemical compositions of base materials and filler metals are shown in Tables 1 and 2. And the main compositions of modified non-corrosive flux are Nocolok flux ($KAlF_4$ and K_3AlF_6 eutectic), Zn and Sn metal powders, etc.

2.2. TIG welding–brazing process

All plates were cut into the size of 200 mm × 50 mm, and the surface was cleaned by abrasive paper and acetone before brazing; a single-V groove was opened in the joint, with a bevel angle of 40° in steel side and 30° in aluminum side. The flux suspension (flux powder dissolved in acetone) was smeared homogenously in a 0.2–0.5 mm thickness on the groove and on both front and back surfaces of the steel in 10 mm width. The schematic of the process is shown in Fig. 1. Aluminum–steel

* Corresponding author. Tel.: +86 451 864 18775; fax: +86 451 864 16186.
E-mail address: sblin@hit.edu.cn (S.B. Lin).

0925-8388/$ – see front matter © 2009 Elsevier B.V. All rights reserved.
doi:10.1016/j.jallcom.2009.08.084

Table 1
Chemical compositions of base materials (wt.%).

Elements	C	Mn	Mg	Al	Si	Cu	Zn	Ti	Ni	Cr	Fe
5A06	–	0.5–0.8	5.8–6.8	Bal.	0.4	0.1	0.2	0.1	–	–	0.4
AISI321	0.12	2.0	–	–	1.0	–	–	0.2	8.0–11.0	17.0–19.0	Bal.

Table 2
Chemical compositions of filler metals (wt.%).

Elements	Si	Fe	Cu	Zn	Mn	Mg	Ti	Al
1100	<0.05	<0.10	<0.10	<0.05	–	–	Bal.	
4043	4.5–6.0	<0.80	<0.30	<0.10	<0.05	<0.05	<0.20	Bal.
4047	11.0–13.0	<0.80	<0.30	<0.20	<0.05	<0.10	–	Bal.

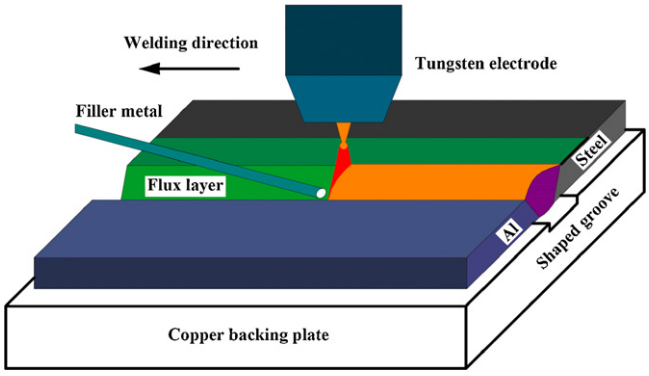

Fig. 1. Schematic of aluminum–steel butt TIG welding–brazing.

butt TIG welding–brazing was carried out by AC-TIG welding source. The welding parameters are welding current 135 A, arc length 3.0–4.0 mm, welding speed 120 mm/min, argon gas flow rate 8–10 L/min.

2.3. Analysis methods

After welding, a typical cross-section of the workpiece was cut and mounted in self-setting epoxy resin in an as-clamped condition. Then the samples were polished to a mirror-like surface aspect and etched with Keller's reagent for 3–5 s. The macrostructures of the joint were observed by optical metalloscope (OM), and the microstructures and compositions of the IMC layers were measured by scanning electron microscopy (SEM) and energy dispersive X-ray spectrometer (EDX). Furthermore, the mechanical properties of the IMC layers were tested in dynamic ultra-microhardness tester and SEM in situ tensile tester. And the fracture surfaces of the joints with different filler metals were analyzed by X-ray diffraction (XRD).

3. Results and discussion

3.1. Shapes and microstructures of IMC layers

Under TIG arc heating, all of the molten filler metals have fully spread on the steel surface to form a sound joint in the wetting action of liquid flux film. Fig. 2 shows the cross-section of the typical

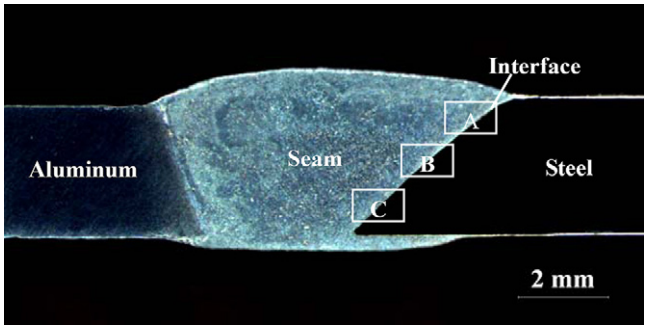

Fig. 2. Cross-section of the aluminum–steel butt joint.

aluminium–steel TIG welding–brazing butt joint with 4047 filler metal. The aluminum alloy sheet and the filler metal are welded, while brazing occurs between the Al-based filler and the steel sheet. At the interface between the Al-based filler and the steel sheet, the IMC layers are formed.

Fig. 3 shows the IMC layers in different positions, plotted by squares in Fig. 2, of the joints with the different filler metals. A very narrow, unequal-thickness interface has formed between welded seam and steel in the brazing process. All the interfaces are mainly made up of two different IMC layers, named the layers I and II from the welded seam to the steel substrate. However, the IMC layers in these joints have great differences in their shapes and microstructures due to the different contents of Si additions in the filler metals.

As shown in Fig. 3a–c, they are the IMC layers in the joint with 1100 pure aluminum filler metal. The I layer in aluminum side presents a long needle-like crystal oriented toward the welded seam, and the II layer in steel side is a compact plate-like phase. Moreover, from the upper part of the interface to the bottom, the needle-like crystal of the I layer fades down due to the lowest heat input at the bottom. So the average interface thickness changes greatly from more than 15 μm at the upper part of the interface to about 5 μm at the bottom.

With adding Si in the filler metal, the shapes and microstructures of the interfaces change drastically. Fig. 3d–f shows the interfaces of the joint with 4043 AlSi5 filer metal. The I layer in aluminum side presents a compact faceted structure, while in steel side the II layer is a small needle-like crystal oriented toward the I layer. The interface thickness is nearly constant and remains in 5–3 μm from the upper part of the interface to the bottom. With the content of Si additions increasing from 5 wt.% to 12 wt.%, the interfaces retain the same shapes and microstructures, as shown in Fig. 3g–i. However, with 4047 AlSi12 filler metal, the interface thickness increases to 8–6 μm from the upper part to the bottom.

From the above results, Si additions have the greatest effect in preventing the build-up of the IMC layer, and minimizing its thickness. However, with increasing the content of Si additions in the filler metal, the solubility of Fe in aluminum molten pool and the dissolution rate of Fe increase greatly. According to previous data on hot-dip aluminizing [11], the solubility of Fe in aluminum bath increases from 5.3 wt.%, 8.7 wt.% to 12 wt.% with the content of Si additions increasing form 0 wt.%, 5 wt.% to 10 wt.% at 800 °C. So, with 4047 AlSi12 filler metal, more Fe atoms dissolve into the molten pool to form thicker IMC layers.

EDS-analyzing results of IMC layers, potted in Fig. 3, of the joints with the different filler metals are shown in Table 3. In the IMC layers with 1100 pure aluminum filler metal, the needle-like I layer in aluminum side is θ-$FeAl_3$ phase and the plate-like II layer in steel side is η-Fe_2Al_5 phase. With the 5 wt.% of Si additions in the filler metal, Si atoms enrich in the interface and participate in the IMC layer formation. Compared with ternary alloy phase diagrams and characteristics of typical Al–Fe–Si system [12–14], the faceted

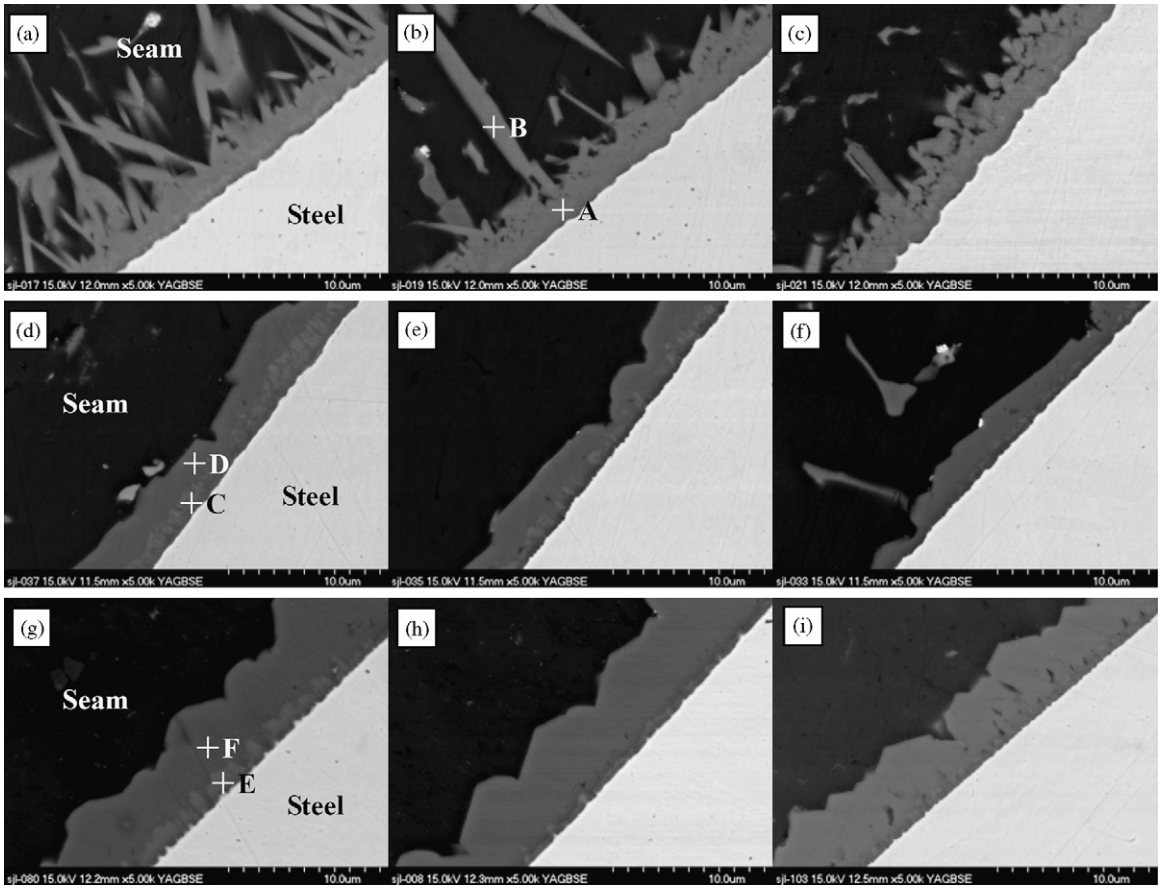

Fig. 3. IMC layers of the joints with different filler metals: (a)–(c) IMC layers in A–C positions, as shown in Fig. 2, of the joint with 1100 filler metal, (d)–(f) with 4043 filler metal and (g)–(i) with 4047 filler metal.

I layer consists of τ_5-$Al_{7.2}Fe_{1.8}Si$ phase, and the needle-like II-layer is θ-$Fe(Al,Si)_3$ phase which dissolves nearly 4.5 wt.% of Si in solid solution. And Si atoms substitute Al atoms of θ-$FeAl_3$ ordered structure. Increasing the content of Si additions to 12 wt.%, the IMC layers consist of the same phases to the layers with 5 wt.% of Si additions. More Si atoms dissolve in θ-$FeAl_3$ in solid solution. At the same time, each layer also contains some contents of Cr and Ni elements from the steel substrate to substitute Fe atoms in IMC layer, which enhance the quality of the layer.

3.2. Mechanical properties of IMC layers

Vicker's microhardness of the IMC layers is measured in dynamic ultra-microhardness tester with 100 mN loading force and 10 s holding time. The average microhardness values of five measurements in each IMC layer are shown in Fig. 4. All the IMC layers are the high-hardness phases. The η-Fe_2Al_5 layer has the highest hardness value, up to 1100 HV, compared with the average 850 HV in the θ-$FeAl_3$ layer of the joint with pure aluminum filler metal.

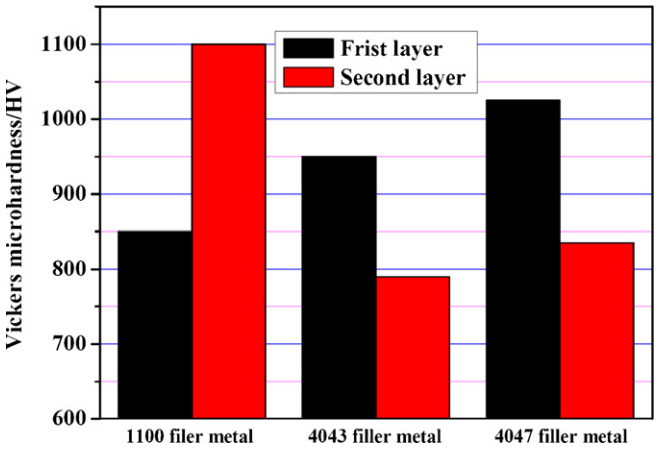

Fig. 4. Microhardness distribution of the IMC layers.

Table 3
EDS analysis results of the IMC layers (wt.%).

Filler metals	Points	IMCs	Al	Si	Fe	Cr	Ni
1100	A	Fe_2Al_5	55.73	–	31.15	07.14	03.08
	B	$FeAl_3$	64.93	–	27.51	02.94	01.82
4043	C	$Fe(Al,Si)_3$	58.36	04.43	29.74	05.50	01.97
	D	$Al_{7.2}Fe_{1.8}Si$	63.54	09.84	21.66	03.58	01.38
4047	E	$Fe(Al,Si)_3$	52.01	09.56	26.37	10.40	00.88
	F	$Al_{7.2}Fe_{1.8}Si$	59.85	10.07	20.37	07.38	01.22

Adding Si elements in the filler metals, the hardness values of the IMC layers decrease greatly. In the interface with 5% of Si additions, the hardness value of τ_5-$Al_{7.2}Fe_{1.8}Si$ layer is 950 HV, compared with 790 HV in the θ-Fe(Al,Si)$_3$ layer. However, with 12 wt.% of Si additions, the IMC layer hardness values are higher than with 5 wt.% of Si additions, which are 1025 HV in the τ_5-$Al_{7.2}Fe_{1.8}Si$ layer and 835 HV in the θ-Fe(Al,Si)$_3$ layer. Most of past reports [13–15] about the solubility of Si in Al–Fe IMC system indicate that Si has a solubility of 0.8–6 wt.% in the θ-$FeAl_3$ phase. When up to 12 wt.% of Si atoms participate in the IMC formation, more Si atoms dissolve in the θ-$FeAl_3$ phase to form the supersaturated solid solution during the rapid cooling which causes the phase hardness increasing.

SEM in situ tensile test was carried out in order to provide a qualitative value of the joint and to analyze the brittleness of IMC layer. The tensile strength of the joints with different filler metals is shown in Fig. 5. The butt joint with 4043 AlSi5 filler metal has the largest tensile strength of 125.2 MPa, compared with 105.0 MPa with 1100 pure aluminum filler metal and 122.5 MPa with 4047 AlSi12 filler metal. And all the joints fracture at the interfaces and the IMC layers are the weak zones of the joints. But with the different filler metals, the fracture occurs at the different positions in the joint interfaces, as shown in Fig. 6. The shapes and microstructures of IMC layers in the interface determine the mechanical properties of the aluminium–steel butt joints. The X-ray diffraction profiles of the fracture surfaces in steel side are shown in Fig. 7. With AlSi5 filler metal, the fracture occurs at the τ_5-$Al_{7.2}Fe_{1.8}Si$ layer, compared to the fractured η-Fe_2Al_5 layer with pure aluminum filler metal and the fractured θ-Fe(Al,Si)$_3$ layer with AlSi12 filler metal.

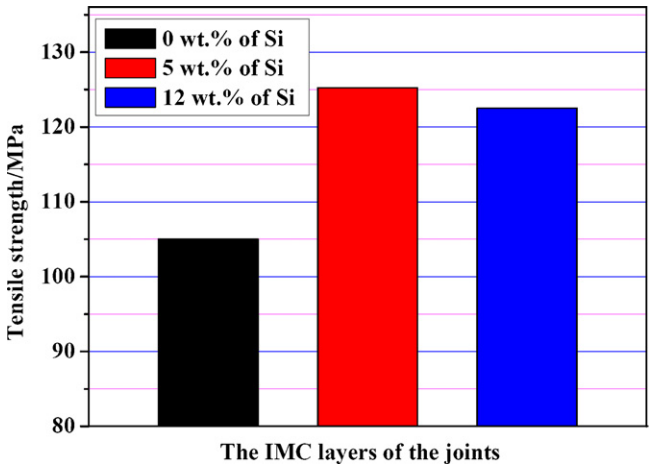

Fig. 5. Tensile strength of the IMC layers.

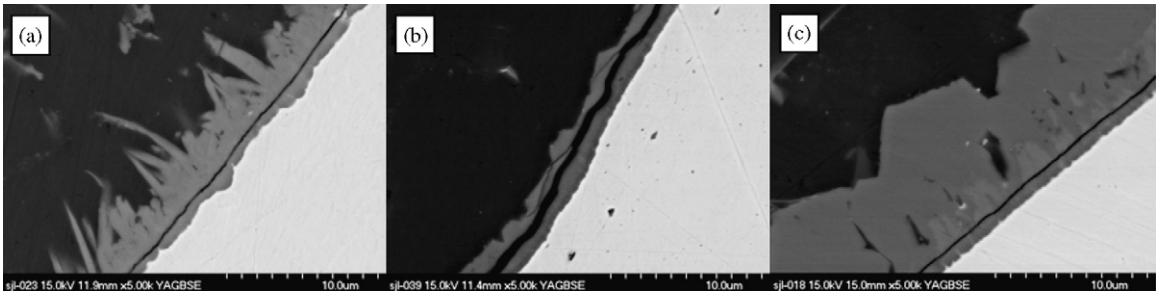

Fig. 6. Cracking positions of the IMC layers under SEM in situ thrust test: (a) 1100 filler metal, (b) 4043 filler metal and (c) 4047 filler metal.

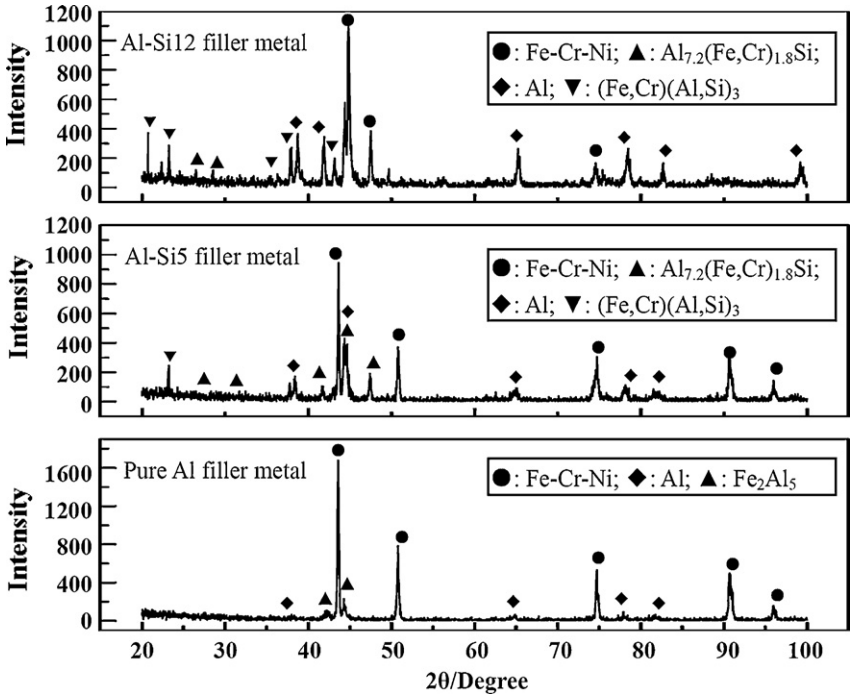

Fig. 7. X-ray diffraction profiles of the fracture surfaces in steel side.

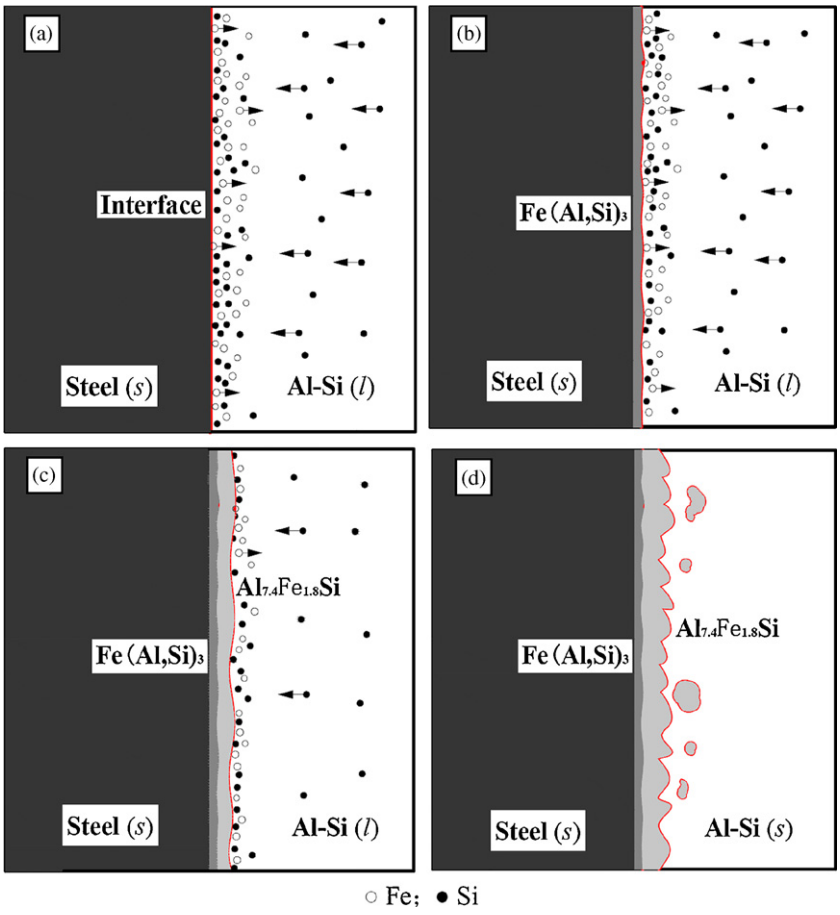

Fig. 8. Growth process of the IMC layers during aluminum–steel TIG welding–brazing with Al–Si filler metals: (a) dissolution and diffusion of Fe and aggregation of Si in the interface, (b) nucleation and growth of θ-Fe(Al,Si)$_3$, (c) Nucleation and growth of τ_5-$Al_{7.2}Fe_{1.8}Si$ and (d) further growth of τ_5-$Al_{7.2}Fe_{1.8}Si$ and solidification of welded seam.

So the tensile strength of the joints shows the tensile property of the different IMC layers. The tensile property of τ_5-$Al_{7.2}Fe_{1.8}Si$ layer is a little higher than that of the η-Fe_2Al_5 layer and the θ-Fe(Al,Si)$_3$ layer.

The results show that 5 wt.% of Si additions in the filler metals can effectively enhance the joining property of the aluminium–steel joint, while adding more Si elements in the filler metal, e.g. 12 wt.% of Si, the tensile strength of the joint does not increase or even decreases, which may be caused by the supersaturated solid solution of Si in the θ-$FeAl_3$ phase. At the same time, the τ_5-$Al_{7.2}Fe_{1.8}Si$ layer is also a hard, brittle phase, which has the limited effect of improving the mechanical properties of the joints. Therefore, in order to improve the quality of the joint greatly, some other elements, e.g. Cu, Zr and La, should be added to the filler metal to improve the ductibility of the IMC layers [16,17].

3.3. Thermal analysis and reaction mechanism of IMC layers

During the aluminium–steel TIG welding–brazing process, the joining temperature is higher than the melting point of aluminum alloy, so the process involves liquid aluminium–solid steel interaction. With Si atoms adding into the filler metal, the phase equilibria and thermodynamic properties of the Al–Fe binary liquid changes greatly.

The formation enthalpy of the IMC layer at 298 K is one of the key data to predict the formation of the IMC layers: the growth of intermetallic phases in the interface and the transition of phases between Al–Fe binary phase and Al–Fe–Si ternary. The formation enthalpy of 1 mole of $Al_xFe_ySi_z$ $(x+y+z=1)$ at 298 K is obtained from the relationship [12–14,17]:

$$\Delta_f H^0_{Al_xFe_ySi_z} = x\Delta_{sol}H^0_{Al} + y\Delta_{sol}H^0_{Fe} + z\Delta_{sol}H^0_{Si} - \Delta_{sol}H^0_{Al_xFe_ySi_z} \quad (1)$$

where $\Delta_{sol}H^0_{Al}$, $\Delta_{sol}H^0_{Fe}$, $\Delta_{sol}H^0_{Si}$ are the respective enthalpies of solution of pure Al, pure Fe and pure Si, $\Delta_{sol}H^0_{Al_xFe_ySi_z}$ is the enthalpy of solution of $Al_xFe_ySi_z$, and x, y, and z are the numbers of moles of Al, Fe and Si atoms, respectively.

The result calculated and measured by Vybornov et al. [17] is that $\Delta_f H^0_{Al_{0.72}Fe_{0.18}Si_{0.1}} = -34,300 \pm 2000$ J/mol. It is lower than the formation enthalpy of 1 mole of Al_xFe_y $(x+y=1)$, which are $\Delta_f H^0_{Al_{5/7}Fe_{2/7}} = 28,805.2$ J/mol and $\Delta_f H^0_{Al_{0.75}Fe_{0.25}} = 27,842.2$ J/mol [17,18]. The result indicates that Si additions can decrease the formation enthalpy of the IMC layers, so in the liquid, Si atoms can aggregate in the interface and participate in the IMC layer's formation.

From the results above, under this type of interaction, five stages are involved, as shown in Fig. 8:

Firstly, the solid steel is wetted and spread by the liquid aluminum in the wetting action of liquid flux film.

Secondly, Fe atoms dissolve into the liquid and subsequently diffuse in the liquid. At the same time, Si atoms aggregate toward the interface (Fig. 8a).

Thirdly, in the interface solidifying process, the θ-Fe(Al,Si)$_3$ phase with a high melting point, more than 1100 °C, nucleates and grows up in steel side (Fig. 8b).

Fourthly, the τ_5-$Al_{7.2}Fe_{1.8}Si$ with a melting point of about 850 °C, nucleates and grows up in aluminum side. The faceted τ_5 is formed

either by the monovariant peritectic reaction, $L + \theta \rightarrow \tau_5$, where the τ_5 phase crystallized along the θ-Fe(Al,Si)$_3$ phase during cooling from the elevated temperature [19], or by the quasiperitectic reaction, $L + \theta \rightarrow \tau_5 + (Al)$ at 620 °C, of the liquid and the θ phase during cooling [11,20]. The τ_5-$Al_{7.2}Fe_{1.8}Si$ phase inhibits the growth of θ-Fe(Al,Si)$_3$ phase, so in the interface with Al–Si filler metal, the θ-Fe(Al,Si)$_3$ phase presents small needle-like (Fig. 8c).

Lastly, the τ_5-$Al_{7.2}Fe_{1.8}Si$ phase subsequently grows up and the τ_5 layer becomes the main layer of the interface. And some irregular block-like τ_5 phases form near the interface in the welded seam (Fig. 8d).

4. Conclusions

(1) Dissimilar metals of 5A06 aluminum alloy and AISI 321 stainless steel were butt joined successfully by TIG welding–brazing with 1100 pure Al, 4043 AlSi5 and 4047 AlSi12 filler metals.
(2) Si additions have the greatest effect in preventing the build-up of the IMC layer, and minimizing its thickness. With 5 wt.% of Si additions, the IMC layer has the optimum mechanical properties.
(3) During the liquid aluminum–solid steel interaction, the growth mechanism of the IMC layers is controlled by dissolution and diffusion of Fe atoms in the liquid. At the same time, Si atoms aggregate in the interface and participate in the IMC layer's formation.

Acknowledgments

The authors would like to thank State Key Laboratory of Welding of China, all of the work within which were conducted. They also appreciate the financial support from the National Natural Science Foundation of China (No. 50874033).

References

[1] M. Staubach, S. Juttner, U. Fussel, M. Dietrich, Weld. Cutt. 7 (2008) 30–38.
[2] R. Qiu, C. Iwamoto, S. Satonaka, Mater. Charact. 60 (2009) 156–159.
[3] J. Song, S. Lin, C. Yang, G. Ma, Y. Wang, China Weld. 18 (2009) 1–5.
[4] K. Hokamoto, K. Nakata, A. Mori, S. Tsuda, T. Tsumura, A. Inoue, J. Alloys Compd. 472 (2009) 507–511.
[5] R.G. Madhusudhan, R.A. Sambasiva, T. Mohandas, Sci. Technol. Weld. Joining 13 (2008) 619–628.
[6] T. Watanabe, H. Sakuyama, A. Yanagisawa, J. Mater. Process. Technol. 208 (2009) 5475–5480.
[7] G. Sierra, P. Peyre, F.D. Beaume, D. Stuart, G. Fras, Mater. Charact. 59 (2008) 1705–1715.
[8] J.L. Song, S.B. Lin, C.L. Yang, G.C. Ma, H. Liu, Mater. Sci. Eng. A 509 (2009) 31–40.
[9] Y. Zhang, Y. Liu, Y. Han, C. Wei, Z. Gao, J. Alloys Compd. 473 (2009) 442–445.
[10] L.A. Jacome, S. Weber, A. Leitner, E. Arenholz, J. Bruckner, H. Hackl, A.R. Pyzalla, Adv. Eng. Mater. 11 (2009) 350–358.
[11] Y.Y. Chang, W.J. Cheng, C.J. Wang, Mater. Charact. 60 (2009) 144–159.
[12] Y. Li, P. Ochin, A. Quivy, P. Telolahy, B. Legendre, J. Alloys Compd. 298 (2000) 198–202.
[13] T. Maitra, S.P. Gupta, Mater. Charact. 49 (2003) 293–311.
[14] Y. Li, P. Ochin, A. Quivy, P. Telolahy, B. Legendre, J. Alloys Compd. 302 (2000) 187–191.
[15] S.W. Pan, F.C. Yin, M.X. Zhao, Y. Liu, X.P. Su, J. Alloys Compd. 470 (2009) 600–605.
[16] D. Chen, Z.H. Chen, J.H. Chen, P.Y. Huang, J. Alloys Compd. 376 (2004) 89–94.
[17] M. Vybornov, P. Rogl, F. Sommer, J. Alloys Compd. 247 (1997) 154–157.
[18] Y. Du, J.C. Schuster, Z.K. Liu, R. Hu, P. Nash, W. Sun, W. Zhang, J. Wang, L. Zhang, C. Tang, Z. Zhu, S. Liu, Y. Ouyang, W. Zhang, N. Krendelsberger, Intermetallics 16 (2008) 554–570.
[19] S.P. Gupta, Mater. Charact. 49 (2003) 269–291.
[20] J. Wang, P.D. Lee, R.W. Hamilton, M. Li, J. Allison, Scripta Mater. 60 (2009) 516–519.